

An Investigation into the Soil Mechanics of Land Anchors

R. J. Godwin; P. N. Wheeler

Department of Agricultural and Environmental Engineering, Silsoe College, Cranfield University, Silsoe, Bedford MK45 4DT, UK

(Received 23 September 1994; accepted in revised form 4 September 1995)

Prediction equations are developed and evaluated to estimate the maximum sustainable pull and the form of penetration of land anchors. The theories for estimating the pattern of penetration and maximum sustainable anchor force compare well with the measured results in five contrasting soil conditions. The maximum and mean error between the predicted and measured maximum anchor force were 13% and 8%, respectively, representing an over-prediction of force in both cases. The correlation coefficient between the maximum anchor force and the mean values of soil shear strength, obtained using the cone index and shear vane were 0.86 and 0.85 respectively indicating that both the cone penetrometer and shear vane are valuable for in-field prediction of maximum anchor forces in both dry frictional and plastic clay soils.

© 1996 Silsoe Research Institute

1. Introduction

Soil anchors, *Fig. 1*, are drawn into the soil surface for a wide range of applications from the classic marine applications for stabilizing both ships and oil platforms for the petrochemical industry, to anchors for assisting in the mobility of vehicles in poor tractive conditions on land. The design of a number of alternative anchors have been studied for use in the petrochemical industry, the majority of these, however, have been simple, empirical “pull” tests in a limited number of soil conditions (Honda and Makamura¹ and Peuch²). Although the performance of anchors has been related to cohesion in clay soils and both submerged unit weight of the soil and operating depth in sandy soils (Peuch²) the maximum sustainable anchor forces have not been found to be predictable using soil mechanics principles. In contrast

Presented at the Second International Conference on Soil Dynamics, Silsoe, Bedford, United Kingdom, 23–27 August 1994

Notation	
γ	Bulk unit weight, kN/m ³
c	Cohesion, kN/m ²
q	Surcharge, kN/m ²
c_a	Adhesion, kN/m ²
ϕ	Angle of internal shearing resistance, deg
δ	Angle of soil metal friction, deg
w	Width of anchor, m
M	Mass of anchor, kg
g	Acceleration due to gravity, m/s ²
x	Width of anchor tips, m
l	Hitch length, m
P	Anchor pull at given depth, kN
H_r	Horizontal component of frictional force between anchor and soil, kN
H_t	Horizontal component of anchor sprag force, kN
V_r	Vertical component of frictional force between anchor and soil, kN
V_t	Vertical component of anchor sprag force, kN
d	Depth of anchor, m
α	Tine rake angle, deg
s	Forward distance travelled, m
y	Implement depth, m
y_e	Equilibrium depth, m
N	Dimensionless number
m	Rupture distance ratio
<i>Suffices</i>	
γ	Gravitational
ca	Cohesive and adhesive
q	Surcharge

to the work of Peuch,² Ahmad³ designed winch anchors using the theory developed by Hettiaratchi and Reece⁴ for predicting passive soil forces but did not conduct an experimental evaluation of his designs.



Fig. 1. Soil anchor used in study

The purpose of this work was to adapt the most appropriate theories developed for soil engaging tools to the performance of soil engaging anchors in a range of soils in terms of the ability of the anchor to both penetrate the soil and to sustain a given pull (P). The benefits of so doing would be to facilitate the prediction of the performance of anchors in various soils, and permit the effects of the geometry, i.e. depth (d), width (w), rake angle (α) and hitch length (l) (see Fig. 2) of the anchor to be evaluated in future designs.

This study was conducted using both theoretical and experimental approaches in the field and laboratory by relating the penetration and anchor force of the anchor, shown in Fig. 1, to a range of soil conditions. The soil physical conditions were assessed using laboratory based measurements of the Mohr-Coulomb soil properties of cohesion (c) and angle of internal friction (ϕ), and which were then used with the force prediction models to calculate the resultant force as the anchor penetrated the soil. Tests of cone penetrometer resistance and shear strength (τ) were made, which enables "in field" estimates of anchor force (P) to be made.

Three field and two laboratory conditions were selected to give a range of soil shear strengths.

2. Theoretical considerations

During the early stages of penetration, Fig. 3 (upper) and Fig. 4 (upper), the anchor behaves as two independent narrow tines of width x , causing two crescent type soil disturbance patterns, i.e. with upward, forward and sideways soil movement as reported by Godwin and Spoor.⁵ At greater depths, Fig. 3 (lower) and Fig. 4 (lower), the independent action

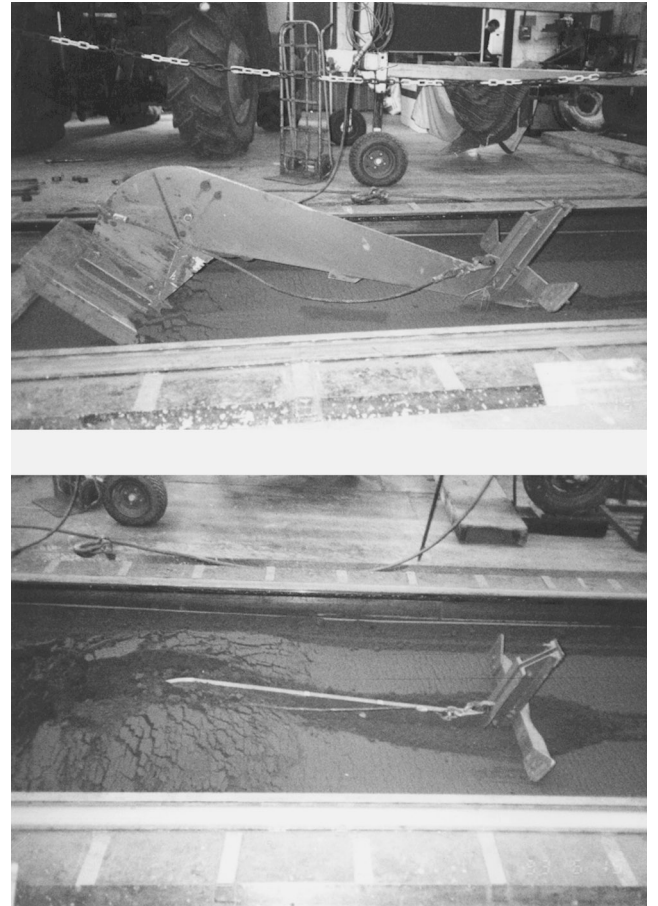


Fig. 3. Initial penetration of anchor (upper) and at equilibrium working depth (lower) in laboratory conditions

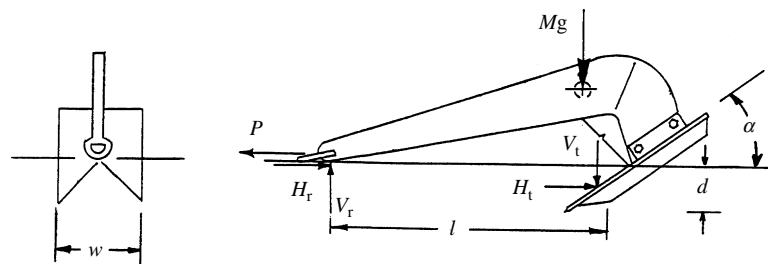


Fig. 2. Free body diagram and principal dimensions of land anchor

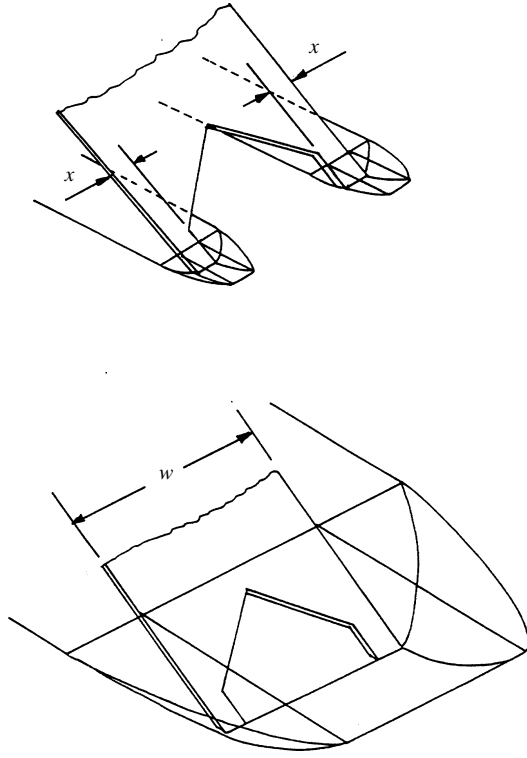


Fig. 4. Soil failure patterns: initial penetration (upper), equilibrium working depth (lower)

of the two points is enveloped by a larger soil failure crescent produced by the width (w) of the anchor behaving as a wide tine (Payne⁶).

2.1. Depth of penetration

The depth of penetration of mole drainage ploughs, for a given forward distance travelled, as recorded by Spoor *et al.*⁷ can be accurately predicted by Eqn (1) developed by Cowell and Sial.⁸ Hence, this approach was considered to predict the depth of penetration (y) of the anchor for a given forward distance travelled

$$y = y_e(1 - e^{-s/l}) \quad (1)$$

where y is implement depth, y_e is equilibrium depth, l is hitch length and s is forward distance travelled. The critical feature of this equation is that the rate of penetration is not affected by the soil condition but only by the hitch length (l) of the implement.

2.2. Soil forces

The forces on the anchor are represented as shown in Fig. 2; where P is anchor pull, at a given depth, H_r is horizontal component of frictional force between

anchor and soil. (This may act either at the front of the shank or further along the shank depending on the depth of penetration), V_r is vertical component of frictional force between anchor and soil, H_t is horizontal component of anchor sprag force and V_t is vertical component of anchor sprag force.

The anchor was pulled using a long cable to minimize any deviations in the direction of the force P from the horizontal. Soil-metal adhesion effects were ignored as they contribute a very small proportion of the total force and were negligible for all the soils tested.

Resolving vertically gives

$$V_r = V_t + Mg \quad (2)$$

By definition the horizontal frictional force

$$H_r = V_r \tan \phi \quad (3)$$

Resolving horizontally gives

$$P = H_r + H_t = (V_t + Mg) \tan \sigma + H_t \quad (4)$$

The force H_t at a given depth of work can be estimated by the passive earth pressure theory developed by Hettiaratchi and Reece⁴ for two-dimensional soil failure and extended for three-dimensional crescent soil failure patterns by Godwin and Spoor⁵ and Godwin *et al.*⁹ as given in Eqn (5). For simplicity it was assumed that the anchor behaved as a blade, as shown in Fig. 4 (lower) over the full depth of penetration rather than assuming that at shallow depths it behaves as two separate tines [Fig. 4(upper)]. Theoretically, this over predicts the force at shallow depths, but this was not considered critical as it was but a transitory position and significant increases in anchor force would result from further increases in penetration depth

$$H_t = (\gamma d^2 N_\gamma + cdN_{ca} + qdN_q) \times \left[w + d \left(m - \frac{1}{3}(m-1) \right) \right] \sin(\alpha + \delta) \quad (5)$$

Similarly the vertical component V_t can be estimated from Eqn (6), after Wheeler and Godwin¹⁰

$$V_t = (\gamma d^2 N_\gamma + cdN_{ca} + qdN_q) \times \left[w + d \left(m - \frac{1}{3}(m-1) \right) \right] \cos(\alpha + \delta) \quad (6)$$

The values of the dimensionless N factors N_γ , N_{ca} and N_q and the rupture distance ratio m (where m is the forward distance of soil treatment from the tine at the surface divided by the depth of the tine) are given

in Hettiaratchi and Reece⁴ and Godwin and Spoor⁵ respectively.

2.3. Example calculation

The following example illustrates the calculations involved when the anchor with mass (M) of 90 kg, is operating at a width (w) of 0.6 m, a depth (d) of 0.5 m and a rake angle (α) of 25° in soil with the properties given in Table 1.

The N factors are from the data in Hettiaratchi and Reece⁴ for a soil-metal friction angle (δ) of 20°.

The following values were substituted into Eqn (5)

$$\begin{aligned} M &= 90 \text{ kg;} \\ \gamma &= 15 \text{ kN/m}^2; \\ d &= 0.5 \text{ m;} \\ N_\gamma &= 1.52; \\ c &= 30 \text{ kN/m}^2; \\ N_{ca} &= 1.79; \\ w &= 0.5 \text{ m;} \\ m &= 2.6; \\ \alpha &= 25^\circ; \\ \delta &= 20^\circ. \end{aligned}$$

Hence

$$\begin{aligned} H_t &= ((15 \times 0.5^2 \times 1.52) + (30 \times 0.5 \times 1.79)) \\ &\times \left(0.5 + 0.5 \left(2.6 - \left(\frac{2.6 - 1}{3} \right) \right) \right) \sin(25 + 20) \\ H_t &= 35.2 \text{ kN} \end{aligned}$$

and similarly from Eqn (6)

$$V_t = 35.2 \text{ kN}$$

Table 1
Mohr–Coulomb and related properties

Quantity	Symbol	Value
Bulk unit weight	γ	15 kN/m ³
Cohesion	c	30 kN/m ²
Surcharge	q	0 kN/m ²
Adhesion	c_a	0 kN/m ²
Angle of internal shearing resistance	ϕ	30 deg
Angle of soil–metal friction	δ	20 deg

The combination of values of rake angle (α) and soil metal friction (δ) used in this example mean that H_t has the same value as V_t .

The total pull P is calculated using Eqn (4)

$$P = (35.2 + 0.9) \tan 20 + 35.2 = 48.3 \text{ kN}$$

To determine the characteristics of the force-depth relationship a computer programme was written with the appropriate N factors included to estimate the anchor force (P), at increasing depths, up to the maximum depth of operation.

3. Experimental investigation

Studies were conducted to determine the rate of penetration and corresponding anchor forces in both the field and laboratory. The anchor was positioned as shown in Fig. 1, on a soil surface, and pulled in the field (at 0.6 m/s) with a 90 kW four wheel drive tractor of mass 7 t, either directly or via a pulley block to double the available tractor pull.

The force was measured using a shear pin dynamometer, the signal from which was recorded in both analogue and digital format. The penetration performance was obtained by making a video recording of the event and by excavating and surveying the disturbed soil profile. Subsequently the penetration depth and analogue force data were synchronized and force/depth relationships obtained.

The laboratory experiments were conducted, at 0.3 m/s, in a 20 m long, 1.5 m wide, 1.0 m deep soil bin where two sandy loam soils ($\gamma = 1.45 \text{ t/m}^3$ and 1.31 t/m^3) were prepared by packing the soil in 50 mm deep layers and rolling each layer to obtain uniform conditions.

The following soil properties were measured for use in the calculations. The values of c and ϕ were obtained from undrained triaxial tests, Bishop and Henkle.¹¹ The values of δ and c_a were obtained by drawing samples of the implement material over the soil at a range of normal loads and recording the horizontal force, after Crowther and Haines.¹²

Measurements of cone index (CI) were made ‘‘in-field’’ using the standard 126.7 mm², 30° cone, ASAE standard S313-1, (Anderson *et al.*¹³) and soil shear strength (τ), using the shear vane, (Aas).¹⁴

In addition to the above properties gravimetric soil moisture contents and bulk density measurements were made. The physical properties of the soils are summarized in Table 2 and the mechanical analyses are presented in Table 3. Two of the field soils were cropped land, while the third soil, the compact sandy loam, was a field track.

Table 2
Physical properties of the soils used in the study

	Field			Laboratory	
	Cultivated sandy loam	Compact sandy loam	Clay	Loose sandy loam	Compact sandy loam
Wet bulk density (ρ) t/m ³	1.75	1.85	1.67	1.31	1.45
Moisture content %d.b.	18.0	14.1	33.5	9.5	9.5
Shear strength* (τ), kN/m ²	68.7	92.8	64.0	28.4	71.6
Cone index* (CI), kN/m ²	1725	2985	1464	737	2016
Cohesion (c), kN/m ²	15	33	27	30	15
Internal friction (ϕ), deg	14	14	8.6	27	30
Adhesion (c_a), kN/m ²	0	0	0	0	0
Soil-metal friction (δ), deg	16.0	19.3	8.6	18.0	20.0

* Mean over the range of depths recorded.

Table 3
Mechanical analysis of soils used in the study

	Sand %	Silt %	Clay %
Sandy loam (Cottenham series*)	72	10	18
Clay (Evesham series*)	4	21	75

* A full description is given in King.¹⁵

4. Results and discussion

4.1. Penetration

Providing the leading edge of the anchor was free from trash, penetration was achieved in all the soils tested, with no sign of the anchor skidding along the surface. The front of the anchor stayed in contact with the ground at all times, as shown in Fig. 2. Typical penetration profiles created by the anchor when entering the soil are shown in Fig. 5 from which it can be seen the final depth reached varied with soil type and condition. The greatest equilibrium depth of penetration of 0.75 m was achieved in the loose sandy loam soil in the laboratory.

Also shown in Fig. 5 are the penetration profiles, as fitted by the model of Cowell and Sial,⁸ which shows that 95% of the equilibrium depth was reached within 4 m of travel when the hitch length (l) was 1.32 m. The measured penetration profiles correspond well with the estimated values especially in laboratory conditions.

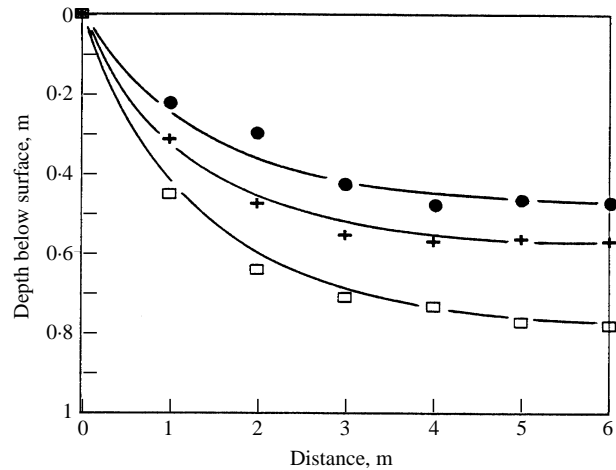


Fig. 5. Penetration depth versus distance travelled in different soils: □, loose sandy loam (laboratory); +, compact sandy loam (laboratory); ●, clay soil (field). Solid lines are those given by Eqn (1) after Cowell and Sial⁸ for the equilibrium depth

4.2. Anchor force versus depth relationship

The force versus depth relationships are shown in Fig. 6 for the five soils. The predicted values are also shown and in all cases the anchor force increased at an increasing rate with working depth. As would be expected (owing to closely controlled soil conditions) the laboratory-based experiments, show closer agreement between predicted and measured values over the depth range than the field-based experiments. The field results showed some deviation between predicted and measured values owing to the variation in soil shear strength with depth. All the predicted values at the equilibrium working depth compared well with those measured, with a mean over-prediction error of

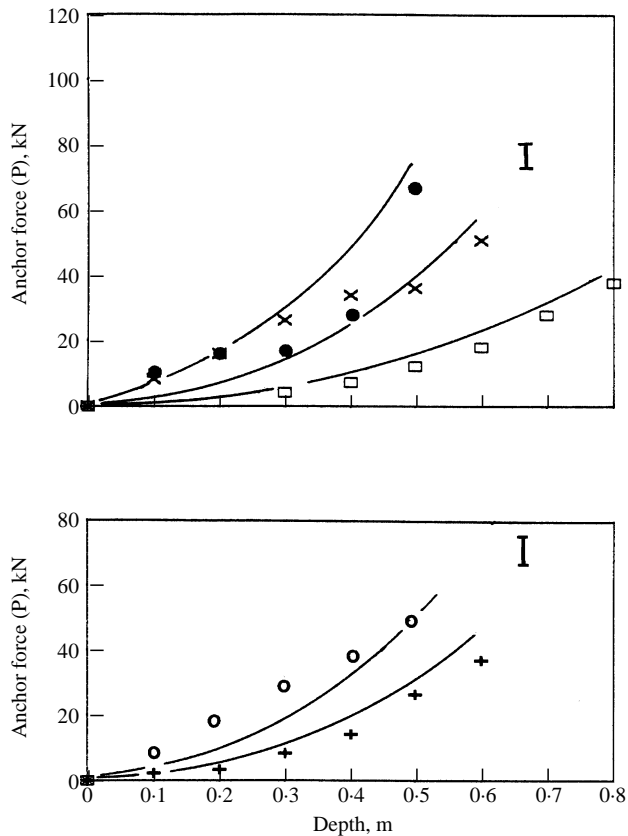


Fig. 6. Force–depth relationships for \square , loose sandy loam (laboratory); +, compact sandy loam (laboratory); \times , cultivated sandy loam (field); \bullet , compact sandy loam (field); \circ , clay soil (field). Solid lines are those predicted for the corresponding soil. Also shown is the l.s.d. at 0.05% probability at maximum sustainable anchor force

8% for all soils. The largest over-prediction error at the equilibrium working depth of 13% occurred in the compact sandy loam.

The predictions illustrate that the anchor force (P) would be significantly increased if the final depth could be increased, hence any modifications which increase the final operating depth of the anchor would be of benefit.

4.3. Anchor force versus cone index and shear strength

The relationship between maximum sustainable anchor force (P), and the mean value of cone index throughout the soil profile down to a depth of 0.5 m for all soils is shown in Fig. 7 (upper). The line on the graph represents the result of linear regression analysis over the working range, with a correlation coefficient (R) of 0.85.

The relationship between the maximum sustainable anchor force (P) and the mean value of shear strength

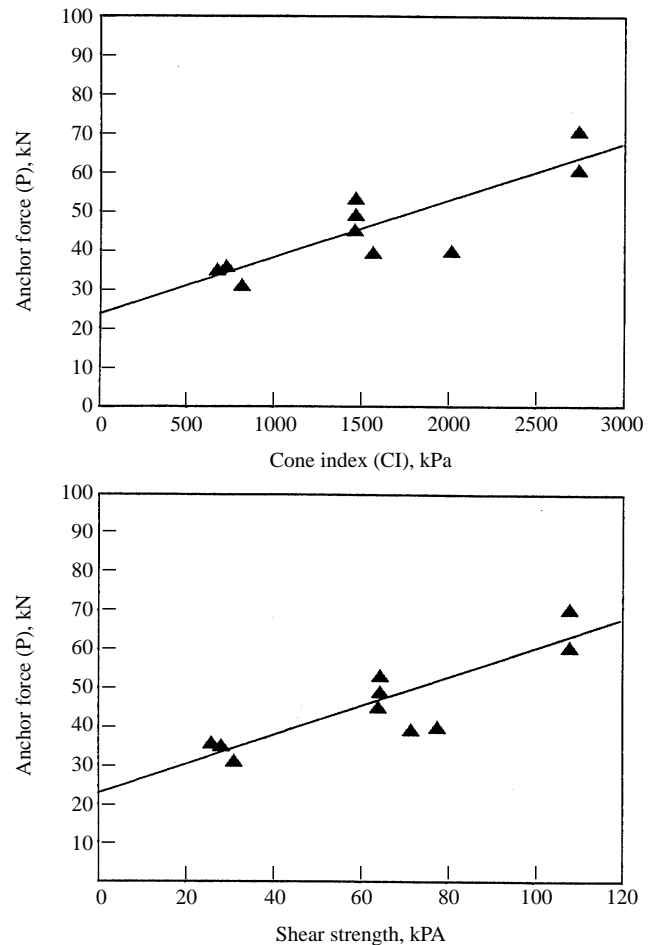


Fig. 7. Relationships between measured maximum sustainable anchor force (P) and the mean value of cone index ($R=0.85$) (upper) and mean value of soil shear strength ($R=0.86$) (lower)

(τ) as measured by shear vane down to a depth of 0.5 m at 50 mm intervals is shown in Fig. 7 (lower). The relationship is very similar to that between force and cone index, with the maximum anchor force (P), increasing linearly with shear strength with a correlation coefficient (R) of 0.86.

5. Conclusions

1. The penetration of the anchor followed a similar pattern for all the soil conditions examined and the distance travelled (approximately 4 m) to reach 95% of the equilibrium depth, followed the pattern of penetration behaviour proposed by Cowell and Sial.⁸

2. The anchor force (P) at the equilibrium working depth, was over-predicted with a maximum error of 13% and a mean error of 8%, from a knowledge of the Mohr–Coulomb soil mechanics properties using

an adapted version of a model developed by Godwin *et al.*⁹ It is reasonable to assume that this model can be used to predict the effects of changing the geometry on the anchor force.

3. Linear correlations coefficients (R) of 0.85 and 0.86 were obtained between the maximum anchor force (P) and the cone index (measured using the standard cone penetrometer) and soil shear strength (measured using the shear vane) respectively in a range of frictional and plastic clay soils. These relationships have practical significance in providing a "quick" method of estimating the maximum anchor force in field conditions.

References

- ¹ **Honda K; Nakamura S** Experimental study of holding power of anchors. Review of Kobe University of Mercantile Marine, Kobe, Japan, 1974, Part 2, (22)
- ² **Peuch A** The Use of Anchors in Offshore Petroleum Operations. Editions Technip, Paris, 1984
- ³ **Ahmad D** A theoretical study on the use of passive soil resistance in winch anchor design. Peranika, 1983, **6**(3): 21–27
- ⁴ **Hettiaratchi H R P; Reece A R** The calculation of passive soil resistance Geotechnique, 1974, **24**(3): 289–310
- ⁵ **Godwin R J; Spoor G** Soil failure with narrow tines. Journal of Agricultural Engineering, 1977, **22**: 213–228
- ⁶ **Payne P C J** The relationship between the mechanical properties of soil and the performance of simple cultivation implements. Journal of Agricultural Engineering, 1956, **1**: 23–50
- ⁷ **Spoor G; Godwin R J; Miller S M** Mole plough grade control. Journal of Agricultural Engineering, 1987, **38**: 145–166
- ⁸ **Cowell P A; Sial F S** A theory for the dynamic behaviour of mouldboard ploughs during penetration. Journal of Agricultural Engineering, 1976, **21**: 313–323
- ⁹ **Godwin R J; Spoor G; Soomro M S** The effect of tine arrangement of soil forces and disturbances. Journal of Agricultural Engineering, 1984, **30**: 47–56.
- ¹⁰ **Wheeler P N; Godwin R J** Soil Dynamics of Single and Multiple Tines at Speeds up to 20 km/h. Submitted to Journal of Agricultural Engineering, in press.
- ¹¹ **Bishop A W; Henkle D J** The measurement of soil properties in the triaxial test, Edward Arnold Ltd., London, 2nd edition 1962
- ¹² **Crowther E M; Haines W B** An electrical method for the reduction of draft in ploughing. Journal of Agricultural Science, 1924, **14**: 221–231.
- ¹³ **Anderson G; Pidgeon J D; Spenser H B; Parks R** A new handheld recording penetrometer for soil studies. Journal of Soil Science, 1980, **31**: 270–296
- ¹⁴ **Aas G** A study of the effect of vane shape and ratio of strain on the measured values of in-situ shear strength of clays. Proceedings of the 6th International Conference on Soil Mechanics, Montreal, Canada, 1965, p141
- ¹⁵ **King D W** Soils of Luton and Bedford District. Soil Survey of England and Wales, Rothamsted, Herts, UK, 1969.